

## CHAPTER 1 - INTRODUCTION

### *1.1 Motivation of Research*

The generation of a robust non-destructive inspection technique involves three primary steps: inspection procedure development, performance validation, and in-field implementation. During the development of a non-destructive inspection procedure, definitions of the data acquisition, signal processing, and feature classification tasks are required. Figure 1.1 shows a typical diagram of a non-destructive inspection procedure displaying these tasks. Data acquisition acquires the raw transducer data based on the prescribed inspection parameters. Signal processing is used to extract the important signal features from the raw transducer data. Feature classification is used to categorize the feature set for the inspection problem. Proper validation of the proposed approach is performed incorporating samples that best represent the variation of flaw characteristics and inspection conditions in the field. Final implementation requires thorough training of inspectors and actual in-field use.

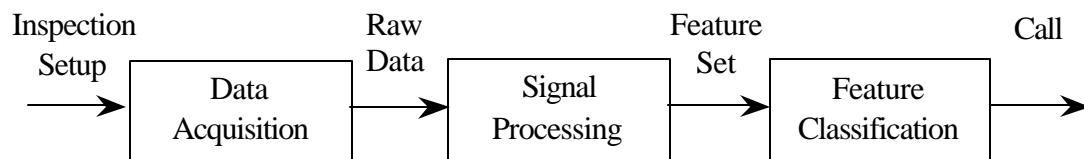


Figure 1.1. Outline for a general non-destructive evaluation procedure.

Typically, non-destructive inspection procedures have been developed empirically. In performing an inspection, engineers and inspectors have often relied on their consistent interpretation of transducer signals. As discussed in this Dissertation, modeling and automation of inspection procedure tasks are two tools that should be increasingly incorporated in the development of non-destructive inspection techniques. Modeling is fundamental to both developing and representing an understanding of the physics of an inspection problem. Automation of the inspection tasks can perform complex calculations both quickly and accurately.

Significant benefit can be gained through incorporating modeling at several stages in the development process [1-4]. Primarily, modeling can be used to generate simulated transducer data as an aid to interpret the raw transducer signals. With this tool, the inspection setup can be adjusted to obtain the desired transducer response. Correspondingly, the model can aid in determining the most robust features for classification. The model can also be used to expand the training set for the signal processing and feature classification tasks, thus improving algorithm performance and reducing experimental sample costs. Modeling has been applied to several complex inspection problems including fatigue cracks, composite materials, and welds [5-8]. Models have also been directly incorporated into feature classification schemes in the form of inverse methods [9]. Improved performance and reduced sample costs may also be achieved during validation through expanding the range of validation samples using

modeling. Models may also be used to display key features of the inspection problem to project sponsors in status reports and to field inspectors during training.

Significant benefit can also be gained through the application of automated classification to the inspection procedure. Primarily, automated classification provides the benefit of improved accuracy, reduced inspector variability, and improved inspection speed realized at the implementation phase. Complex signal processing and feature classification tasks can be efficiently performed using automated procedures [10-11]. During the development phase, automated classification naturally leads to automating the algorithm development process. Automated training in conjunction with neural networks has been applied to non-destructive inspection procedure development [12-13]. The training of neural networks using both simulated and experimental data has been demonstrated [14-15].

As non-destructive inspection problems become more challenging, the benefit of modeling and the application of automated classification during the development process becomes more evident. As an example, quantitative evaluation approaches are used to determine the geometry of flaws in order to determine the remaining life of the part. To achieve this challenging goal, a greater need for proper modeling and robust automated classification is evident. In this Dissertation, a particular class of inspection problems, namely, the ultrasonic inspection of C-141 weep holes and C-141 rib clip holes, where the combination of modeling and automated classification can be applied to the development process to gain significant benefit, has been investigated in detail.

Weep holes are incorporated in the risers of wing structures in C-141 aircraft in order to allow fuel to be properly distributed during flight. Figure 1.2 shows a diagram of a weep hole in a C-141 wing section. The C-141 inner wing contains over 700 weep holes. These holes give rise to stress concentrations that can lead to fatigue cracks. Two cases of fatigue cracks have been observed emanating from weep holes, top cracks which propagate upward and bottom cracks which propagate downward toward the wing surface. Due to the location of top cracks relative to the external surface of the wing, conventional ultrasonic techniques have difficulty in detecting their existence. In addition, small bottom cracks may be obscured within the specular reflection from the hole. Currently, bolt hole eddy current (BHEC) inspection is carried out as a routine depot maintenance process to determine the condition of the inner wing weep holes. The BHEC inspection requires fuel tank entry by the inspection technicians and is a costly and time-consuming process. Successful implementation of an automated ultrasonic inspection technique from the outside of the wing eliminates the fuel tank entry requirement and drastically reduces weep hole inspection costs for the Air Force.

Prior work has shown the benefit of a two-element ultrasonic transducer technique for the generation and measurement of circumferentially creeping Rayleigh waves around the weep hole to determine the existence of top cracks [16-17]. For implementation of this promising method as a robust protocol, a number of challenges remained to be overcome. First, the laboratory procedure does require considerable care in assessing the A-scan signals for top crack detection. The 'leaky' Rayleigh wave signal

must be separated from the preceding specular signal and from the noise signals generated by the geometry of the system. Second, locating the weep holes and the means of positioning the transducers for bottom and top crack detection must be added to the protocol. To reduce the likelihood of operator error in conducting these tasks, an automated technique for the analysis of the signals for both bottom and top crack detection remained to be developed.

Following detection of a fatigue crack, characterizing the size of the crack is important in defining the proper corrective action. For notch sizes smaller than 0.070 in., resizing the hole in order to remove the flaw is feasible. For notch sizes 0.070 in. and larger, a patch or replacement of the panel is required. Accurate determination of the crack length would be valuable toward selecting the required diameter to remove the flaw and streamline the process for the addition of a patch or the replacement of a panel section.

Current weep hole inspection requires that the wet wing be completely purged of fuel before inspection can begin. Due to the time and cost of emptying and drying out a wing, the capability of weep hole inspection for a wing containing fuel is of interest to the Air Force. Prior work has been performed to understand the effect of a fluid-filled cavity on the performance of the two-element weep hole inspection technique for radial fatigue cracks [18-21]. These papers indicated significant challenges for directly applying the dual transducer weep hole inspection approach for top crack detection. Models of the scattering response for an incident shear wave transducer signal and for the

case of fluid-filled cavities with radial fatigue cracks would provide insight into a viable ultrasonic inspection strategy.

Another factor that may affect the performance of the ultrasonic inspection technique is a polyurathane coating on the inside edge of the C-141 weep holes. This coating is used to protect the edge of the hole from corrosion. The current procedure requires that the coating be removed prior to inspection. A significant reduction in time and effort would be gained by eliminating the need for the removal and the subsequent reapplication of this coating. The development of a model would generate the needed understanding in order to assess the viability of using the weep hole inspection procedure for this case.

Currently, the Air Force is initiating development of an ultrasonic technique for the detection of fatigue crack in holes containing fasteners. Two field examples are the C-141 rib clip holes and the C-130 beam cap holes. These two cases are similar to the C-141 weep hole case in that they are located within a riser with access limited for an ultrasonic transducer to a single wing side. The first issue that must be addressed in developing an ultrasonic inspection approach for cylindrical holes containing elastic inserts is to characterize the interface conditions between the hole and the fastener. Following characterization of the interface, a model is necessary to investigate the viability of signals for top crack detection. The nature of the waves propagating about the interface should be explored. Lastly, an understanding of the sensitivity of the

inspection technique to variation in measurement, geometric and material parameters is needed.

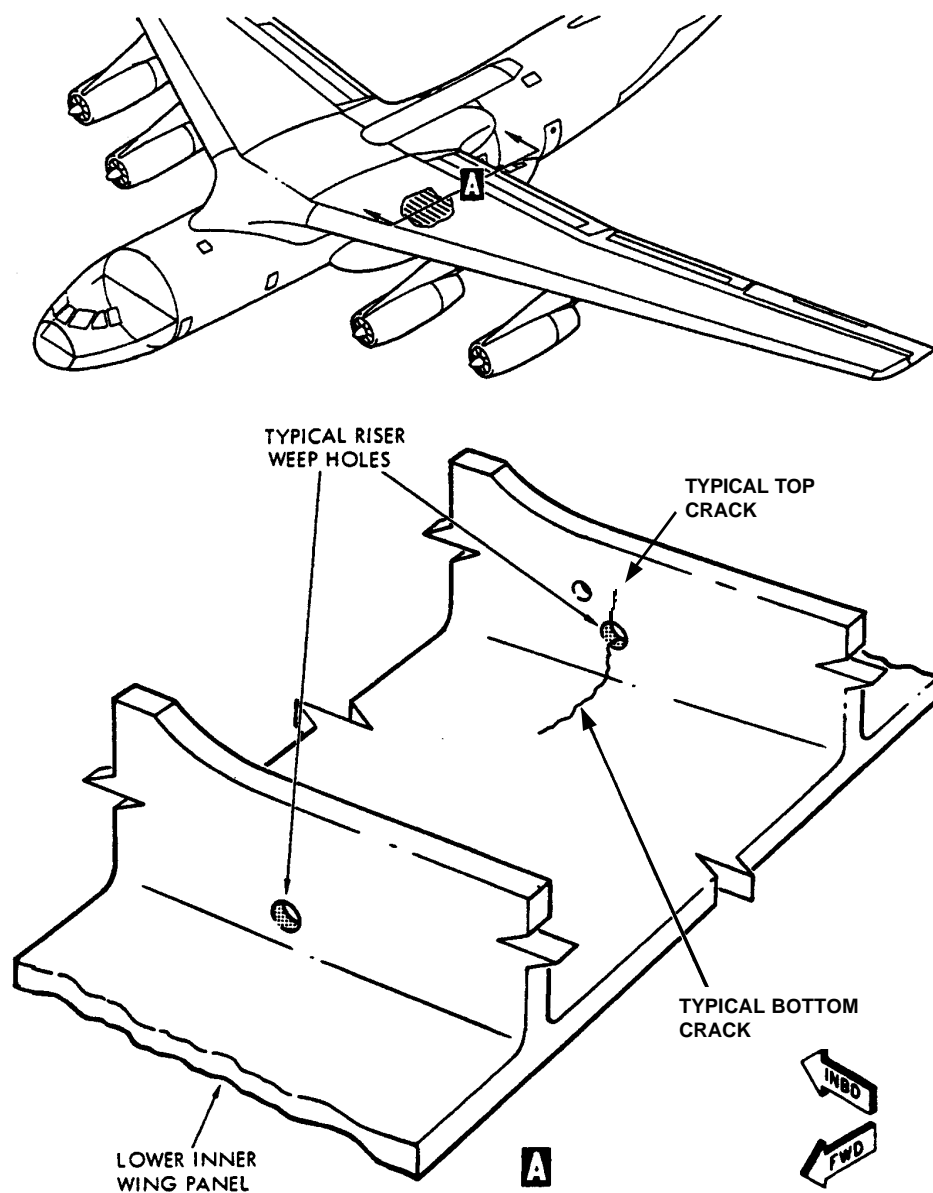


Figure 1.2. Diagram of location of weep holes [22].

## *1.2 Summary of Work*

This Dissertation provides solutions to the problems discussed in Section 1.1 that had been unresolved or undefined in previous work. Figure 1.3 displays a diagram of the inspection problems that have been addressed. Ultrasonic non-destructive evaluation (NDE) for radial fatigue cracks was investigated for four cylindrical hole configurations: the empty cylindrical hole, the fluid-filled cylindrical hole, the cylindrical hole containing an elastic layer, and the cylindrical hole containing an elastic insert. Due to constraints on the placement of the transducer relative to the cylindrical cavity, special NDE techniques were explored for the possible detection and sizing of cracks at the bottom and top locations. Each study, organized by chapter, is categorized in Figure 1.3 according to the hole configuration, the crack location and the classification type, detection or sizing, addressed.

Bottom crack detection by viewing C-scan images obtained through pulse-echo ultrasonic inspection was found to miss certain small cracks. To better understand the transducer response for the ultrasonic inspection problem, a model was developed to simulate the A-scan signals and the also corresponding B-scan and C-scan maps. A 2D boundary element method (BEM) simulation was formulated for the total field response for an incident ultrasonic transducer signal by a cylindrical hole with a surface breaking crack or notch. A technique was developed which examines the variation in the A-scan signals as the transducer is incrementally moved along the wing surface across the region



of a weep hole. This spatial signal variation (SSV) approach for multiple signal classification is presented in Chapter 2. Studies of both experimental and simulated BEM signals were used to develop this approach. The advantage of this refined B-scan classification technique is the ability to detect superimposed signals independently from the general shape of the generated transient pulse.

Chapter 3 describes the implementation of a neural network assisted, automated ultrasonic inspection technique for bottom and top crack detection of weep holes. Toward achieving the goal of field implementation of an automated inspection technique, this work demonstrates the value of numerical simulation, laboratory studies and algorithm training with samples representing in-field variation, in-field demonstration, parametric sensitivity studies, and probability of detection (PoD) validation. The inspection capability of the automated procedure was found to exceed both the defined inspection requirements and the ability of inspection through viewing C-scan images. In addition, the automated neural network approach only requires scanning from one direction while the C-scan approach requires scanning from both directions. Thus, the automated neural network approach provides a significant improvement in both detectability and inspection time over the C-scan approach.

No prior work was found which investigated the effect of curvature on the reflection and transmission of Rayleigh waves by surface breaking cracks. Ray analysis, analytical models and boundary element method (BEM) simulations were used to understand the nature of ‘secondary’ reflected and transmitted signals from notches on a

cylindrical hole. From these results, a methodology for sizing top notches is presented in Chapter 4. The capability of the procedure to detect small notches and to differentiate between various notch sizes is discussed.

Chapter 5 presents a study examining the possibility of top notch detection for fluid filled weep holes. A BEM model was formulated for the scattering response of an incident shear wave transducer signal by a fluid-filled hole with a fluid-filled notch. A viable ultrasonic inspection strategy was developed from the results of the simulations. Validation of the approach is presented for both simulated and experimental top-notch data.

An analytic model was derived for a plane incident shear wave upon a cylindrical hole with an elastic layer. Solutions for the dispersion relations and the transient response to a plane shear wave incident on the hole were used to investigate the effect of a polyurathane coating on the inside surface of the C-141 weep holes. The results of this study are presented in Chapter 6.

Chapter 7 presents a study examining the possibility of top crack detection for holes containing elastic inserts. A BEM model was formulated for the scattering response of an incident shear wave transducer signal by a cylindrical hole with a radial notch, an elastic insert, and a stiffness interface between the hole and the insert. Through comparisons with experimental data, characterization of the interface condition between the hole and the insert was determined. A feasible ultrasonic inspection strategy was determine from the simulated and experimental studies. Validation of the approach is

presented for both simulated and experimental data. An examination of the sensitivity of the inspection technique to variation in measurement, geometric and material parameters is also presented.

<p><b>Case A) Empty Hole</b></p>	<table border="1"> <thead> <tr> <th colspan="2">Bottom Crack</th> </tr> </thead> <tbody> <tr> <td>1) Detection</td> <td><a href="#">Chapter 2-3</a></td> </tr> <tr> <td>2) Sizing</td> <td>-</td> </tr> <tr> <th colspan="2">Top Crack</th> </tr> <tr> <td>1) Detection</td> <td><a href="#">Chapter 3</a></td> </tr> <tr> <td>2) Sizing</td> <td><a href="#">Chapter 4</a></td> </tr> </tbody> </table>	Bottom Crack		1) Detection	<a href="#">Chapter 2-3</a>	2) Sizing	-	Top Crack		1) Detection	<a href="#">Chapter 3</a>	2) Sizing	<a href="#">Chapter 4</a>
Bottom Crack													
1) Detection	<a href="#">Chapter 2-3</a>												
2) Sizing	-												
Top Crack													
1) Detection	<a href="#">Chapter 3</a>												
2) Sizing	<a href="#">Chapter 4</a>												
<p><b>Case B) Fluid-Filled Hole</b></p>	<table border="1"> <thead> <tr> <th colspan="2">Bottom Crack</th> </tr> </thead> <tbody> <tr> <td>1) Detection</td> <td>-</td> </tr> <tr> <td>2) Sizing</td> <td>-</td> </tr> <tr> <th colspan="2">Top Crack</th> </tr> <tr> <td>1) Detection</td> <td><a href="#">Chapter 5</a></td> </tr> <tr> <td>2) Sizing</td> <td>-</td> </tr> </tbody> </table>	Bottom Crack		1) Detection	-	2) Sizing	-	Top Crack		1) Detection	<a href="#">Chapter 5</a>	2) Sizing	-
Bottom Crack													
1) Detection	-												
2) Sizing	-												
Top Crack													
1) Detection	<a href="#">Chapter 5</a>												
2) Sizing	-												
<p><b>Case C) Elastic Layer</b></p>	<table border="1"> <thead> <tr> <th colspan="2">Bottom Crack</th> </tr> </thead> <tbody> <tr> <td>1) Detection</td> <td>-</td> </tr> <tr> <td>2) Sizing</td> <td>-</td> </tr> <tr> <th colspan="2">Top Crack</th> </tr> <tr> <td>1) Detection</td> <td><a href="#">Chapter 6</a></td> </tr> <tr> <td>2) Sizing</td> <td>-</td> </tr> </tbody> </table>	Bottom Crack		1) Detection	-	2) Sizing	-	Top Crack		1) Detection	<a href="#">Chapter 6</a>	2) Sizing	-
Bottom Crack													
1) Detection	-												
2) Sizing	-												
Top Crack													
1) Detection	<a href="#">Chapter 6</a>												
2) Sizing	-												
<p><b>Case D) Elastic Insert</b></p>	<table border="1"> <thead> <tr> <th colspan="2">Bottom Crack</th> </tr> </thead> <tbody> <tr> <td>1) Detection</td> <td>-</td> </tr> <tr> <td>2) Sizing</td> <td>-</td> </tr> <tr> <th colspan="2">Top Crack</th> </tr> <tr> <td>1) Detection</td> <td><a href="#">Chapter 7</a></td> </tr> <tr> <td>2) Sizing</td> <td>-</td> </tr> </tbody> </table>	Bottom Crack		1) Detection	-	2) Sizing	-	Top Crack		1) Detection	<a href="#">Chapter 7</a>	2) Sizing	-
Bottom Crack													
1) Detection	-												
2) Sizing	-												
Top Crack													
1) Detection	<a href="#">Chapter 7</a>												
2) Sizing	-												

Figure 1.3. Four hole conditions investigated for ultrasonic NDE of cracks (notches).